Molecular BioSystems

Accepted Manuscript

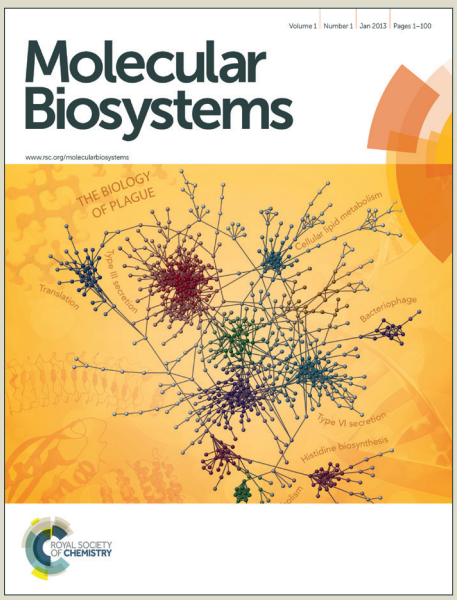

ROYAL SOCIETY OF CHEMISTRY

www.rsc.org/molecularbiosystems

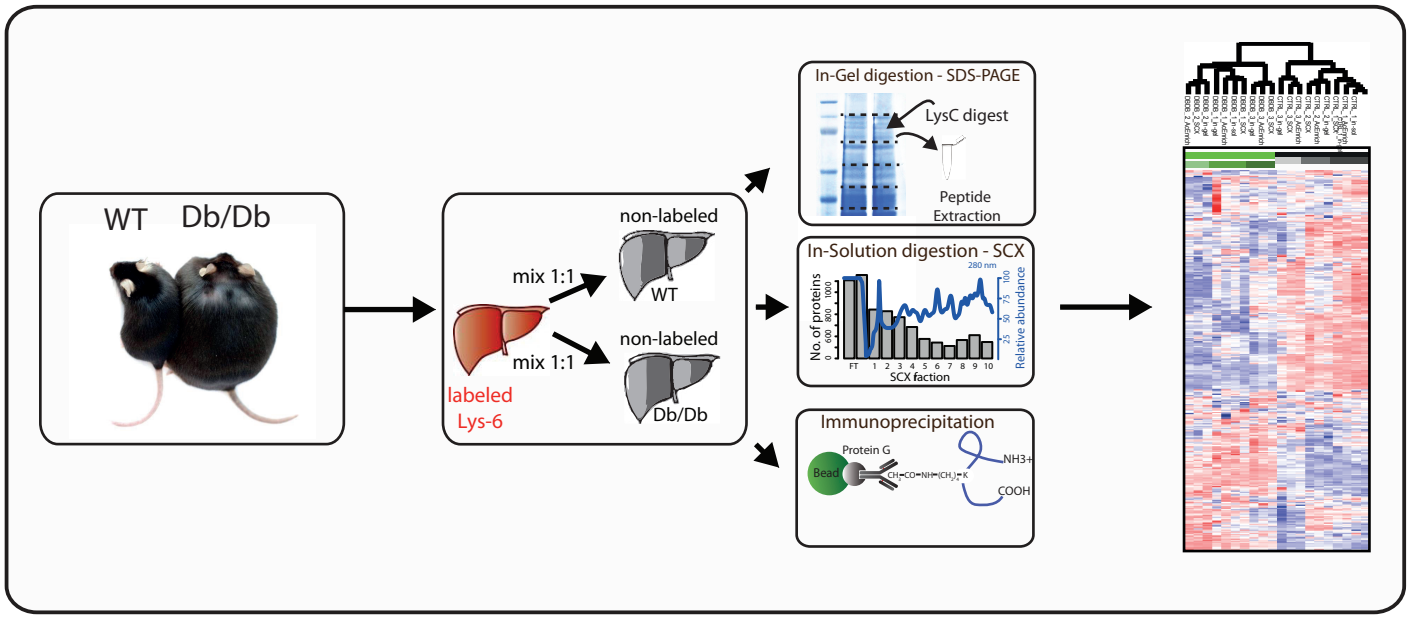

In-vivo SILAC-based quantitative proteomics approach to analyse protein abundances and acetylation levels under diabetic conditions.

Dissection of metabolic pathways in the Db/Db mouse model by integrative proteome and acetylome analysis

Soraya Hölper[†,a], Hendrik Nolte [†,a,#], Eva Bober [a], Thomas Braun [a] and Marcus Krüger [a,b,#]

Insulin resistance is often associated with excessive caloric intake and metabolic syndrome (MS) favours development of Diabetes Mellitus Type II (T2DM). T2DM is a chronic disease with severe long-term consequences such as dyslipidemia, retinopathy, kidney failure, and cardiovascular diseases. Although studied extensively, several aspects of T2DM remain poorly understood. Liver is the leading organ in the maintenance of metabolic fitness serving as the first relay station for processing dietary information in a direct response to nutritional input and changes in insulin and other endocrine signals. Evidence from several murine models suggests a unique function of the liver in development of MS and T2DM. Here, we utilised Db/Db mice to understand the impact of T2DM on the proteome of liver cells. Global analysis of the liver proteome using SILAC approach identified 407 significantly regulated proteins under diabetic conditions out of 8500 identified liver proteins. Furthermore, we mapped 1604 different acetylation sites in liver proteins. After normalization on the protein level, we identified 34 regulated acetyl lysine residues on 21 individual proteins, which were significantly altered in Db/Db compared to wildtype livers. We reason that the dataset provides a versatile resource for functional studies aiming to understand consequences of changes in protein abundances and acetylation in livers of diabetic animals.

Received 00th January 2014,
Accepted 00th January 2014

DOI: 10.1039/x0xx00000x

www.rsc.org/

Introduction

The liver is a multifunctional organ which integrates metabolism of carbohydrates, ketone bodies and lipids. This metabolic control is exerted by a plethora of cytoplasmic and mitochondrial enzymes making the liver a key organ for the whole body homeostasis. Food intake raises blood sugar level, which is normalized by a rapid secretion of the growth hormone insulin by β-cells in the pancreas. Subsequently, insulin-induced receptor activation results in an increased glucose transport and metabolism in target tissues, such as liver, skeletal muscle, and adipose tissues[1, 2]. This balanced system of insulin secretion and sugar uptake is disturbed when the insulin production from β-cells is defective or peripheral tissues do not respond properly to the insulin signal. This insulin resistance (IR) is promoted by various environmental and genetic risk factors[3] and is frequently associated with an increased body weight[5]. IR results in hyperglycaemia, dysregulated lipid synthesis, and an increased glucose production (gluconeogenesis). A prolonged insulin dysfunction leads to development of Diabetes mellitus type2 (T2DM). As a consequence of the long-term high glucose levels and overweight, Diabetes patients often develop cardiovascular diseases, atherosclerosis, diabetic retinopathy, and kidney failure. The causal interrelationship between obesity and development of IR is still not completely understood but a rich body of literature indicates a close molecular interplay between adipocytes, immune- and liver cells[6]. Secreted molecules from the fat tissue such as adiponectin, leptin, proinflammatory cytokines, and lipids are crucial to control the metabolism of hepatocytes[7]. Inadequate adipocytes-governed secretion in obese individuals may affect insulin response resulting in changed phosphorylation level of several insulin signaling molecules such as the insulin receptor itself, the insulin receptor substrates (IRS-1/2), and the AKT kinase, and thus lower insulin sensitivity and liver function[8, 9].

Another factor important for proper liver function is the mitochondrial metabolism. The activity of mitochondria is not only essential for energy production, but also for other processes like the urea cycle, the pentose phosphate pathway, ketone body synthesis, and lipid metabolism. There is growing evidence that mitochondrial dysfunction plays a major role for the induction of insulin resistance[10]. For example, increased levels of fatty acids and ceramides

caused by an impaired mitochondrial ß-oxidation negatively affect the phosphorylation level of insulin-activated signaling molecules, such as IRS-1 and contribute to the insulin resistance phenotype[10, 11]. Interestingly, acetylation of lysine residues of a large number of mitochondrial metabolic enzymes plays a pivotal role to modulate the activity of mitochondrial pathways[12].

The Db/Db (diabetes/diabetes) mouse strain, which has a mutation in the leptin receptor[13] represents an excellent experimental model system to study the development of IR and subsequent metabolic activities underlying diabetes. This mouse model is characterized by an early onset of obesity and progressing hyperglycemia[14] leading finally to hepatic steatosis, IR and diabetes[15, 16]. Recently, several large-scale microarray and deep sequencing studies of diabetes models demonstrated dysregulation of several metabolic genes and enabled an unbiased and systematic analysis of the IR phenotype[4, 17, 18].

In addition to those global transcriptome studies, large-scale analyses of protein abundances and their posttranslational modifications (PTMs) have advanced our knowledge of signaling pathways under regular and perturbed conditions. Mass spectrometry based proteomics revealed post translational modifications, such as phosphorylation, acetylation, methylation and ubiquitination for virtually all metabolic enzymes and signaling molecules. As mentioned above, several studies found a strong correlation between lysine acetylation and enzymatic activities of mitochondrial proteins. For example, acetylation of the key mitochondrial enzyme of the ketone body synthesis pathway, the 3-hydroxy-3-methylglutaryl CoA Synthase (Hmgcs2) is important for its increased enzymatic activity during fasting[19]. The fatty acid oxidation enzyme Enoyl-coenzyme A hydratase (Ehhadh) is also acetylated/deacetylated at differing conditions.

However, the biological relevance of most of the detected modifications in the presently available datasets remains elusive, because most studies fail to quantify proteins and their modification sites in a condition-specific manner. Moreover, it was recently shown that lysine acetylation in mitochondria is most likely driven by non-enzymatic reactions, since the high acetyl-CoA content in mitochondria is sufficient to promote this reaction. Therefore, it is necessary to accurately quantify protein abundances and levels of acetylated peptides to reveal condition-dependent expression changes and to distinguish between background and regulated acetylation sites.

Here, we used an in-vivo SILAC-based quantitative proteomics approach to analyse protein abundances and acetylation levels in liver tissue of wild-type and Db/Db animals at the age of approximately 4 months under steady state conditions. These experiments were performed in biological triplicates using three different separation techniques which resulted in the identification of more than 8500 liver proteins and 6200 of them were quantifiable. Further, among of the total detected 1604 lysine acetylation sites, only a minor fraction of 34 acetylation sites on 21 proteins appeared to be regulated. The here generated dataset confirmed protein changes due to increased fatty acid levels and the insulin resistance phenotype. On the other side, in obese Db/Db animals a limited set of peptides with an altered acetylation was observed as compared to lean control animals.

Results and discussion

Spike-in of SILAC liver tissue revealed dynamic protein expression in Db/Db animals

The aim of our experiments was to perform a global proteome and acetylome analysis of insulin resistant liver tissue from obese Db/Db mice compared to lean wild-type animals under steady-state conditions. The inactivation of the leptin receptor leads to an increased food uptake and, at the approximately two months of age, an excessive accumulation of visceral adipose tissue. Clearly, chronic obesity leads to higher free fatty acid (FFA) levels in the periphery and results in the modulation of several metabolic pathways in different cellular compartments, including mitochondria, endoplasmatic reticulum, peroxisomes, and microsomes. To perform an accurate protein and peptide quantification of the complex liver tissue we used a spike-in SILAC approach to quantify proteins and acetylated peptides upon an acetyl-lysine enrichment step. Liver proteins from Lys6 labeled SILAC-mice were used as an internal protein standard[20] and mixed equally with non-labeled liver from wild-type (n=3) and non-labeled liver from Db/Db animals (n=3) (**Figure 1A**). Protein extracts were digested with LysC. As a first analytical set we performed in-gel digestion of three individual livers from wild-type and Db/Db animals each (independent biological triplicates, n=3). To maximize the protein coverage we used in a second analytical set the same lysates and for in-solution digestion and SCX chromatography (n=3). In a third set, we combined in-solution digestion with 4h liquid chromatography gradients (n=1) (**Figure 1B**). In total, we measured 326 peptide fractions by LC-MS/MS using a nano-UHPLC equipped with a 50 cm reversed phase column connected to a QExactive (Thermo Fisher Scientific) mass spectrometer via a nano-spray ionization source. For the enrichment of acetylated peptides we performed an immunopurification step using an acetyl-lysine antibody (Immunechem). Protein and acetyl peptide ratios from Db/Db and control livers were then compared ('ratio of ratio') and the acetyl fold

change was normalized to protein differences (**Figure 1C-E**).

The high overlap between technical replicates (Pearson correlation 0.87-0.95) reflects the accurate and highly confident SILAC quantification across different sample preparations and separation techniques (**Suppl. Figure 1**). Since we used the SILAC mouse liver as an internal protein standard we calculated the direct DbDb/WT ratio by dividing the SILAC ratios heavy/WT and heavy/DbDb. Finally, the direct DbDb/WT ratios revealed an average correlation of 0.66 (**Figure 2A**). In total, we quantified 4146 protein ratios using at least two different techniques and quantified 2608 protein ratios from the overlap of all three experiments (**Figure 2B, Suppl. Table 3**).

Among the 2608 quantified proteins 747 mitochondrial proteins were detected, which reflects the metabolic activity of the liver and covers ~68% of all Mitocarta entries. The ratio distributions of mitochondrial proteins were similar to the ratio distribution of the whole proteome (**Figure 2C**). Notably, 22% of the identified mitochondrial proteins were found to be acetylated.

To determine whether the SILAC ratios of control and Db/Db animals could be grouped into subunits we used hierarchical clustering of 335 control and Db/Db proteins, which were quantified in all experiments. The clustering revealed clear segregation of clusters between wild-type and Db/Db animals. However, we also detected differences within the wild-type and Db/Db group (**Figure 2D**), indicating biological variability between individual animals of the control and Db/Db group, respectively.

Nevertheless, principal component analysis covering 46.8% and 23.0% of the total variance revealed also a clear segregation between both groups (**Figure 2E**). To deal with the multiple-testing problem in high

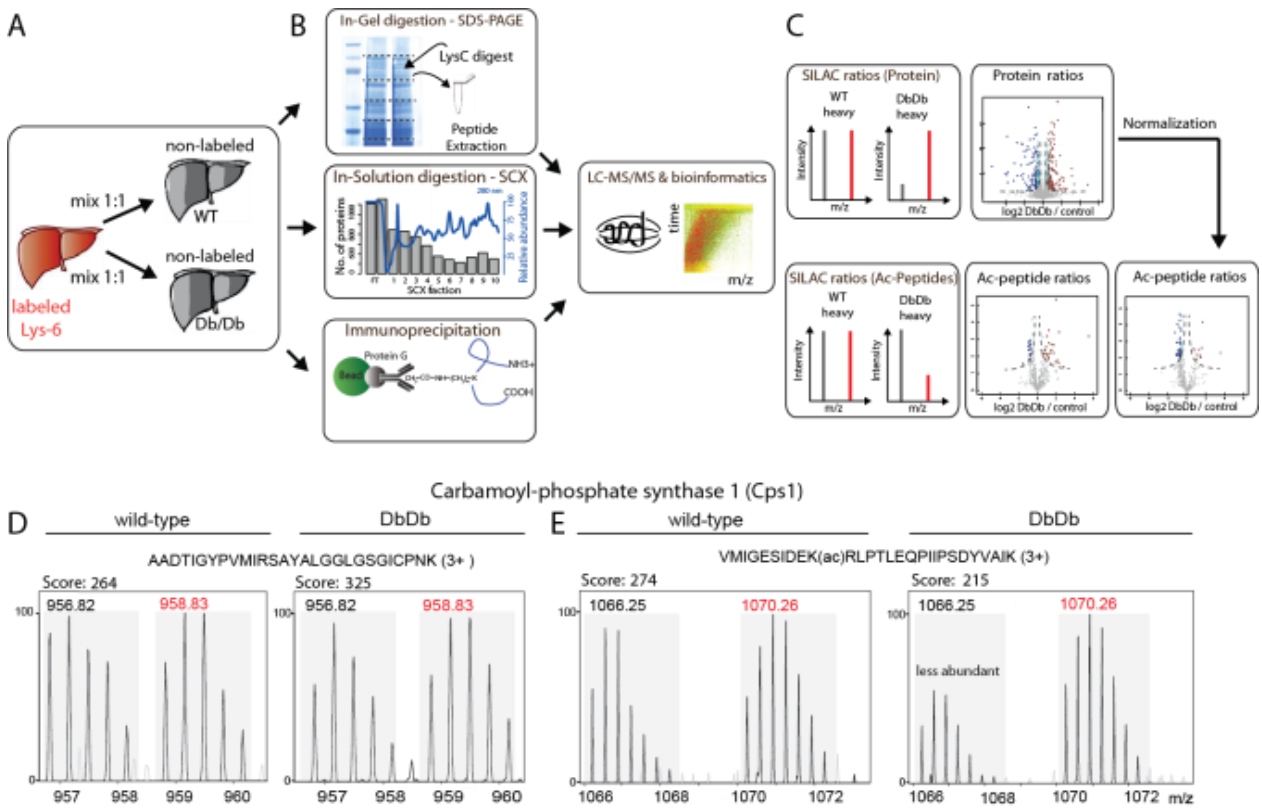

Figure 1: Quantitative proteome and acetylome analysis of Db/Db mice liver (A) Experimental design for the analysis of Db/Db and control mice. Liver proteins from both Db/Db and control mice were mixed with heavy liver proteins from the SILAC mouse. (B) Acetylated peptide enrichment: digested lysine-acetylated peptides were enriched using anti-acetyl lysine antibody (Immunechem). In-depth proteome analysis was carried out by in-gel digestion and in-solution digestion coupled to SCX chromatography for peptide separation. The resulting peptides were then analyzed by high-resolution LC-MS/MS (C) Protein and acetyl peptide ratios from Db/Db and control livers were then compared ('ratio of ratio'). (D-E) Examples showing the relative acetyl fold change for Carbamoyl-phosphate synthase 1 (Cps1). The protein quantification was based on the unmodified peptides and was used for normalizing the acetyl peptides fold changes.

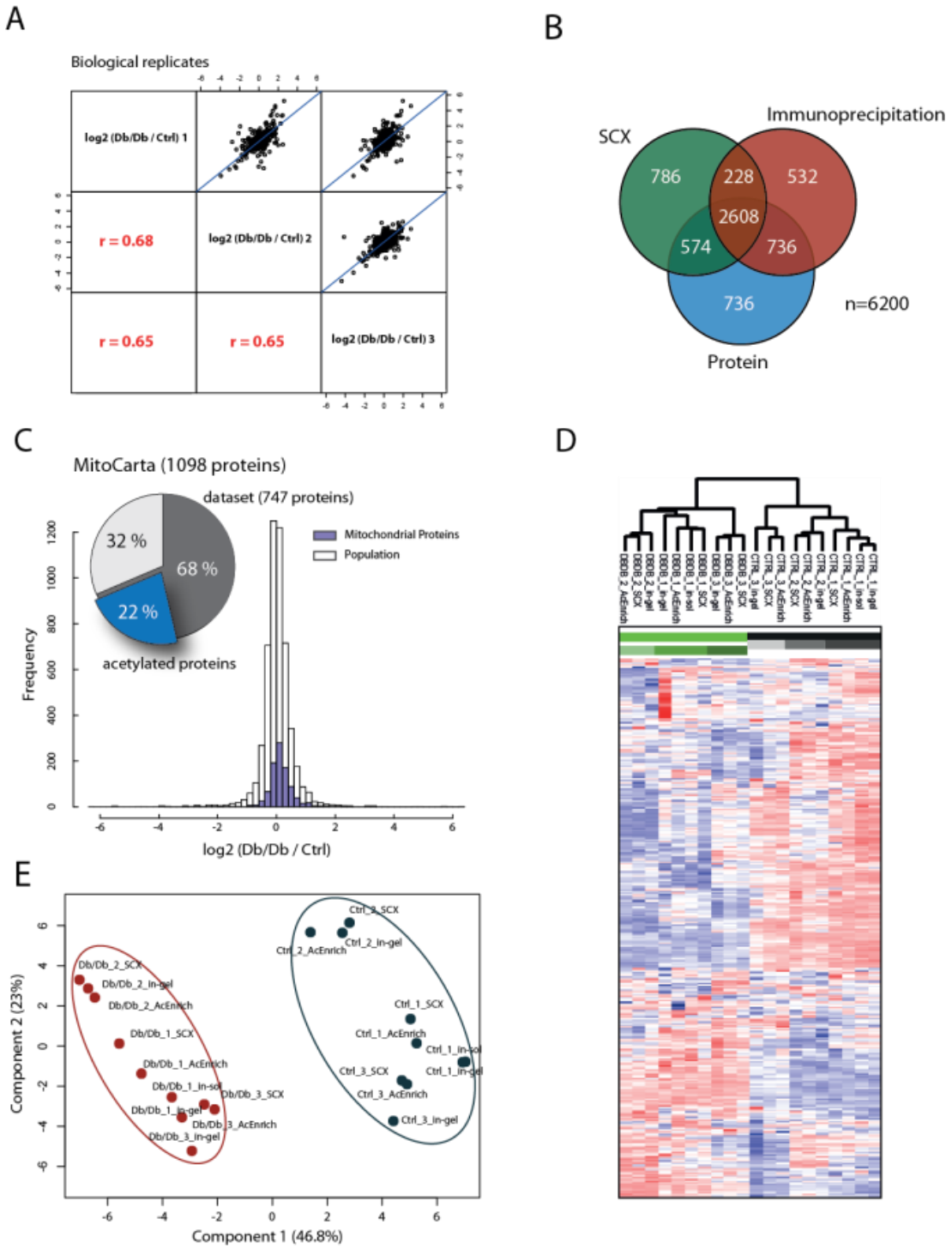

Figure 2: Experimental results of proteome analysis of Db/Db mice (A) The comparison of the biological replicates of the direct DbDb/Control ratio for each experiment revealed an average correlation of 0.66. (B) A total of 6200 proteins are quantified. Venn diagram indicated an overlap of 2608 proteins quantified in each technique. (C) Quantification of 747 mitochondrial proteins which covers ~68% of all Mitocarta entries. Approximately 22% of all Mitocharta entries were found to be acetylated. The ratio distributions of mitochondrial proteins are similar compared to the ratio distribution of the whole proteome. (D) Hierarchical clustering of 335 Db/Db and control ratios results in a separation of clusters differing in their expression profiles. (E) Principal component analysis covering 47% and 23% of the total variance revealed also a clear segregation between both groups.

throughput techniques and identification of significant differently expressed proteins we performed permutation based FDR calculation algorithm within the SAM (Statistical analysis of microarray) approach and identified 407 significantly regulated candidates between Db/Db and control mice. 237 of these candidates exhibited a fold change higher than 1.5 (**Figure 3A and B**). Next, we performed Fisher exact test on the level on Gene Ontology and KEGG pathway annotation to compare significantly regulated proteins (FDR threshold 0.05 and fold change 1.5) against all identified proteins. Our data revealed protein expression changes in several important metabolic pathways, including Fatty acid metabolism, PPAR signaling, and branched chain amino acid (BCAA) degradation as the most significantly enriched KEGG pathways (FDR below 10e-6) (**Figure 3C**). To integrate mRNA and protein abundances we overlapped our proteomic dataset with a recent sequencing dataset of Db/Db animals[4]. In total, we found ~3500 overlapping candidates with a Pearson correlation of 0.35 (**Figure 3D**) and taken only the fraction of regulated candidates into account we observed a Pearson correlation of 0.6 (data not shown). Taken together, the SILAC based proteomic approach generates high confidence data due to the good reproducibility.

Proteome profiling shows metabolic adaption to increased free fatty acids in Db/Db animals

To prevent excessive fatty acid levels and subsequent lipotoxicity the liver has developed several transporters, binding proteins and enzymes to rapidly deplete and metabolize free fatty acids from the body[21]. In accordance with previous reports we also monitored increased levels in several mitochondrial transporters, beta-oxidation enzymes, and carbohydrate enzymes in Db/Db animals (**Figure 4, Suppl. Table 3**). Below, we list several examples of the most prominent regulated enzymes in the Db/Db liver involved in the uptake, transport, and in the activation of fatty acids.

Uptake and transport of fatty acids are increased in Db/Db animals

We found Cd36 and the Low-density lipoprotein receptor (Ldlr) as most significantly up-regulated proteins in Db/Db liver tissue. Cd36 also known as fatty acid translocase (Fat) is a scavenger membrane protein that binds and transports fatty acids. The general Cd36 inactivation in mice leads to decreased fatty acid uptake and hypoglycemia, whereas its overexpression in the muscle tissue leads to enhanced fatty acid oxidation and hyperglycemia[22, 23]. Thus, an increased level of Cd36 seems to be an adaptive response to higher fatty acid levels in the body (**Suppl. Table 4**).

Transport of organic anions across the cell membrane is regulated by solute carrier organic anion (Slco) family members. We observed a drastically reduced protein level of Slco1a1 (fold change 0.07) in Db/Db mice while other Slco´s such as Slco1a4 and Slco1b2 were not changed as compared with the lean control. Notably, the Slco1a1 reduction was also observed previously at the mRNA level in Db/Db and Ob/Ob animals[24].

Another important class of transporters is the ATP-binding cassette transporter family (Abc transporters). Members of this protein class facilitate the transport of drugs and endogenous substances such as cholesterol and fatty acids through plasma and intracellular membranes. Here, we observed a slight down-regulation for the transporters Abca1 and Abcc6, whereas the transporters Abcd1 (also known as adreno-leukodystrophy protein, Aldp) and Abcd3 were up-regulated in Db/Db animals. Abcd1 transporters are localized within peroxisomal membranes and are responsible for the transport of very-long-chain acyl-CoAs into the peroxisome. A dysfunction of the Abcd1 leads to a beta-oxidation defect and an accumulation of very long-chain fatty acids[25]. Moreover, it has been shown that peroxin 19 (Pex19), known as an important protein for peroxisomal membrane synthesis, interacts with Abcd1. Consequently, we found also an increased Pex19 protein level in Db/Db animals. Thus, it is likely, that increased levels of a subset of peroxisomal transporters modulate the conversion of specific fatty acids for energy production. In contrast, the quantification of fatty acid transport proteins (Fatp also known as Slc27a) revealed no changes between wild-type and Db/Db animals.

Surprisingly, the insulin receptor itself did not show changes on protein level. However, we detected several other factors such as the inhibitory factor receptor (Lifr) and the cell adhesion molecule activated leukocyte molecule (Alcam) to be clearly down-regulated, indicating other pathways affected by the insulin resistance phenotype. However, the direct association and participating signaling molecules between those pathways remain elusive.

Finally, we quantified several fatty acid binding proteins (Fabp), which regulate the transport of lipids to different compartments in the cell. We found increased levels of Fabp2 and Fabp4 in Db/Db animals. Notably, the most abundant liver fatty acid binding proteins Fabp1 and Fabp5 (also known as epidermal Fabp) were significantly down-regulated in Db/Db animals, indicating different cellular functions among the Fabp family members.

Differential modulation of long-chain fatty-acid-coenzyme A ligases (Acsl) for the activation of free fatty acids in Db/Db animals

After the uptake and transport to different compartments fatty acids are activated by acyl-CoA ligases (Acsl) through a conversion from free long-chain fatty acids to fatty acyl-CoA esters. Solubilized acyl-CoA´s are then utilized as substrates for beta-oxidation and for conversion to triacylglycerides and membrane phospholipids. We detected Acsl1, 3, 4, 5 expression in liver tissue and found a clear down regulation of Acsl1 and Acsl4 in Db/Db animals (**Figure 4, Suppl. Table 4**). However, previous high fat diet experiments revealed an opposite effect and showed increased levels of Acsl1 mRNA expression in liver of Zucker obese rats (fa/fa)[26]. Notably, a recent deep sequencing study showed that the mRNA expression of Acsl1, Acsl4, and Acsl5 were not changed in Db/Db liver[4]. Moreover, another report showed an opposite regulation of Acsl1 and Acsl4 protein and mRNA levels. They observed that fasting for 48h decreased the Acsl1 protein abundance in liver whereas the mRNA level increased[27] (**Suppl. Table 3**). Thus, the discrepancy between mRNA and protein levels upon altered metabolic conditions, such as high fat diet, fasting, chronic obesity, and insulin resistance clearly indicates distinct translational and posttranslational regulations for members of the Acsl family.

Activated fatty acids are subsequently transported into mitochondrial and peroxisomal compartments via carrier systems. We found increased levels for the carnitine palmitoyl transferase 2 (Cpt2), the solute carrier proteins Slc25a15/20 (also known as Mitochondrial ornithine transporter 1) and the Carnitine O-acetyltransferase (Crat) in Db/Db animals. In addition, we measured also increased protein levels in Db/Db animals for virtually all beta-oxidation enzymes and connected pathways reflecting again the higher metabolic activity of liver mitochondria due to increased food uptake and higher fatty acids content (**Figure 4**). However, we did not observe any changes on mitochondrial respiratory protein complexes (complex I-V) in Db/Db animals. The consequence of high rates of fatty acid oxidation is an increase in acetyl-CoA in mitochondria and an excess of acetyl-CoA is transferred to the TCA cycle and the ketone body synthesis. Here, we found several proteins of those pathways, including Acat1, Hmgcs2 and Hmgcl, which were highly enriched in Db/Db animals.

Taken together our results are consistent with previous studies describing the adaption of lipid uptake, transport and activated metabolic pathways in obese and insulin resistance Db/Db animals.

Biotransformation and microsomal omega oxidation

The next group of significantly changed metabolic enzymes comprised several dysregulated detoxifying enzymes of the P450 and glutathione S-transferase (Gst) family. These protein families are essential for the biotransformation of toxins and neutralisation of the reactive oxygen species. Gst and members of the cytochrome P450 family play a crucial role in the resistance to carcinogens, antitumor drugs, and oxidative stress[28].

An additional function of cytochromes is the hydroxylation of the terminal carbon atom (omega) of fatty acids within microsomes. Although the omega oxidation is only a minor pathway in the fatty acid metabolism as compared to mitochondrial and peroxisomal beta-oxidation, it seems that this pathway acquires an important role under certain physiological conditions such as diabetes and alcohol consumption. We found a ~10 fold increase of cytochrome P450A10 and P450A14 in Db/Db livers. Conversely, the P4502C70 and P4503A11 showed a ~4 fold decreased level. In addition to cytochrome P450, it was shown that impaired levels of specific Gst´s, including Gstt1, Gstm1 and Gstp1 were associated with type 2 diabetes in humans[29]. Here we identified seven Gst´s (Gsta2, Gstm1, Gstm2, Gstm3, Gstm4, Gstt3, Gstk1) to be up-regulated in Db/Db liver and the most abundant liver glutathione Gsta2 also showed the highest up-regulation (fold-change of ~3.5).

Altogether, the detection of differentially expressed subsets of cytochrome P450 and Gst´s in Db/Db animals reflects the adaptation to an increased oxidative stress in compartments such as mitochondria, microsomes and peroxisomes.

Carbohydrate metabolism

The storage and utilization of glycogen is an important pathway to provide energy for the whole body. The key regulators of glycogen metabolism are the hormones insulin and glucagon. Several studies showed that adult Db/Db animals have increased sugar levels and a severe hyperglucagonemia. However, the overall hepatic glycogen level is obviously not changed[14]. The breakdown of hepatic glycogen (glycogenolysis) is catalyzed by the glycogen phosphorylase (Pygl), the rate limiting enzyme for the sequential removal of sugar molecules. Our analysis revealed only slightly increased Pygl levels in Db/Db animals. We observed a significant up-regulation of several key enzymes of the glycolysis/glycogenolysis such as the fructose-1,6-bisphosphate, the glucose-6-phosphatase, and the glucokinase/ hexokinase in Db/Db animals (**Figure 5, Suppl. Table 3**).

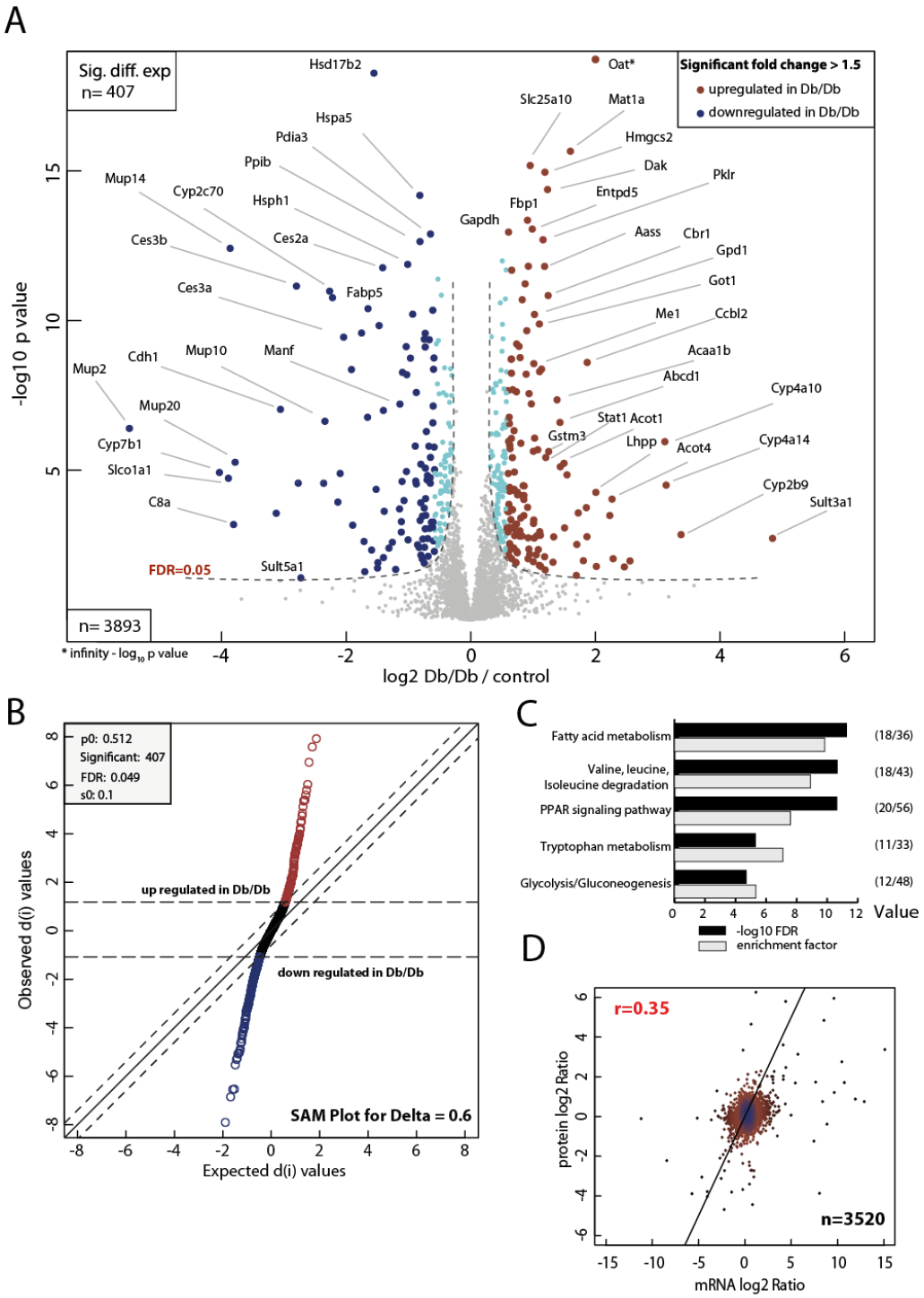

Figure 3: (A) Volcano plot of log2 ratios representing the log2 fold change of Db/Db to control mice. Significant differently expressed proteins are colour coded: red indicates >1.5 fold change, blue shows down-regulated proteins (<1.5 fold change) and teal represents all proteins with lower absolute fold changes. Performing permutation based FDR calculation algorithm within the SAM (Statistical analysis of microarray) approach identified 407 regulated candidates between Db/Db and control mice while 170 exhibit no significant fold changes (FDR threshold 0.05, indicated by dashed line). (B) SAM Plot: Dashed lines represent Delta cut-off within the SAM statistic leading to an FDR of 0.05 excessed by a fudge factor s0 of 0.1 and a calculated posterior probability of 0.5. (C) Identification of significantly enriched KEGG pathways by Fisher Exact test using all quantified proteins as a reference database. The regulated proteome is enriched for metabolic pathways. Graph shows the Benjamini Hochberg corrected p-value for selected metabolic pathways. (D) Correlation of our proteome and a recent published mRNA dataset of Db/Db animals [4] showing a Pearson correlation of 0.35. Overlap was performed using gene name annotation.

Amino acid conversion

Another pathways important for energy supply are the conversion and breakdown of amino acids. For example, the pyridoxal enzymes, alanine aminotransferase (Alt also known as Gpt) transfers the alpha amino group from glutamate to pyruvate to form alanine in muscle tissue. Alanine is then absorbed by the liver to generate pyruvate via the aminotransferase reaction. Here we found a ~two-fold increase of Gpt2 (Alt2) in Db/Db mutant liver tissue, while the Gpt1 isoform was not changed, indicating that only Gpt2 was induced in the liver of Db/Db mutants. Similar results have been shown for the Gpt1/2 gene expression levels in liver of Ob/Ob animals[30]. Another aminotransferase is the aspartate aminotransferase cAST (also known as Got1). We found an increased protein abundance only for the cytosolic isoform in Db/Db mice, whereas the mitochondrial isoform mAST (Got2) was not affected. In contrast to Gpt2 and Got1, the level of the Gamma-glutamyltransferase 1 (Ggt1) was not changed. Further changes in expression of several enzymes involved in the catabolism of amino acids, which provide metabolites such as pyruvate, acetyl-CoA, Succinyl-CoA, and Ketoglutarat for the TCA cycle and ketone body synthesis were observed. Among others, argininosuccinate synthase (Ass1), branched chain ketoacid dehydrogenase E1 (Bckdha/b), the S-adenosylmethionine synthase (Mat1a), the serine dehydratase (Sds), and the urocanate synthase (Uroc1) were up-regulated in Db/Db animals.

Signaling molecules

In addition to insulin signaling, which mainly regulates carbohydrates and fatty acid metabolism in the liver, other signaling pathways are also involved in the regulation of enzymatic activities and are important for the maintenance of the liver homeostasis. Recently, it has become evident that inflammatory pathways are activated by metabolic stresses such as lipid overload and increased glucose levels. Thus, an unbalanced energy homoeostasis has a direct impact on the immune system and is described as a para-inflammatory event [31]. Our study identified increased levels of several kinases, including the ribosomal protein S6 kinase (Rps6ka1), the Aurora kinase B (Aim1), and the macrophage activating kinase Sedoheptulokinase (Shpk) in Db/Db animals. Further evidence of activated inflammatory pathways comes from the elevated levels of Stat1, the interferon downstream effector Interferon-induced guanylate-binding protein 2 (Gbp2), and two interferon inducible GTPases (ligp1 and lgtp), which were also increased in Db/Db animals. The increased expression of Stat1 and Acot2 were confirmed by immunoblot (**Figure 6A**).

It has been shown that down-regulation of epidermal growth factor receptor (Egfr) leads to diabetes since the receptor act as a key player for the development of a functional pancreatic β-cells[32]. In addition, several studies showed a beneficial effect of Egfr inhibition in adult diabetic mice due to down-regulation of oxidative stress[33]. Here we observed by mass spectrometry and immunoblot a decreased expression of EGF receptor in Db/Db animals compared to lean controls (**Figure 6A**).

Further, we found down-regulation of several ribosomal proteins, export proteins (Signal peptidase complexes), N-Glycan biosynthesis proteins, selenium binding proteins, and extracellular coagulation cascade proteins in Db/Db animals (S**uppl. Table 3**).

Taken together, the in vivo SILAC approach enabled us to accurately profile liver proteins and to identify 407 highly dynamic and significant candidates to be regulated in Db/Db animals. Besides the detection of regulatory constituents of several metabolic pathways we have also identified signaling proteins, protein export mechanisms, and secreted proteins which were regulated in animals with Diabetes Mellitus Type 2 phenotype.

Chronic obesity in Db/Db animals leads to minor changes of acetylation levels under steady state conditions

Dynamic phosphorylations have been proven to be important in the regulation of virtually all cellular pathways.

For example, the reversible phosphorylation of mitochondrial proteins is a key mechanism to regulate ketogenesis during the onset of type 2 diabetes[34]. Recently, several global acetylome studies showed that dynamic protein acetylation on lysine residues is also a key post-translational modification to modulate metabolic enzymes[35,36]. It was shown that specific deacetylases such as Hdac´s and Sirtuins play important roles in triggering enzymatic activity, stability and substrate specificity. For example, the inactivation of Sirt3 results in profound changes of acetylation levels on mitochondrial proteins, which modulate activity of several metabolic pathways[37, 38, 39].

Here, we used an acetyl-lysine immunopurification for the enrichment of acetylated peptides in Db/Db mutants. We performed in solution digestion with trypsin, because acetylated lysine is not accessible by this protease. Hence, peptides with a C-terminal arginine, which contain a modified lysine are available for SILAC

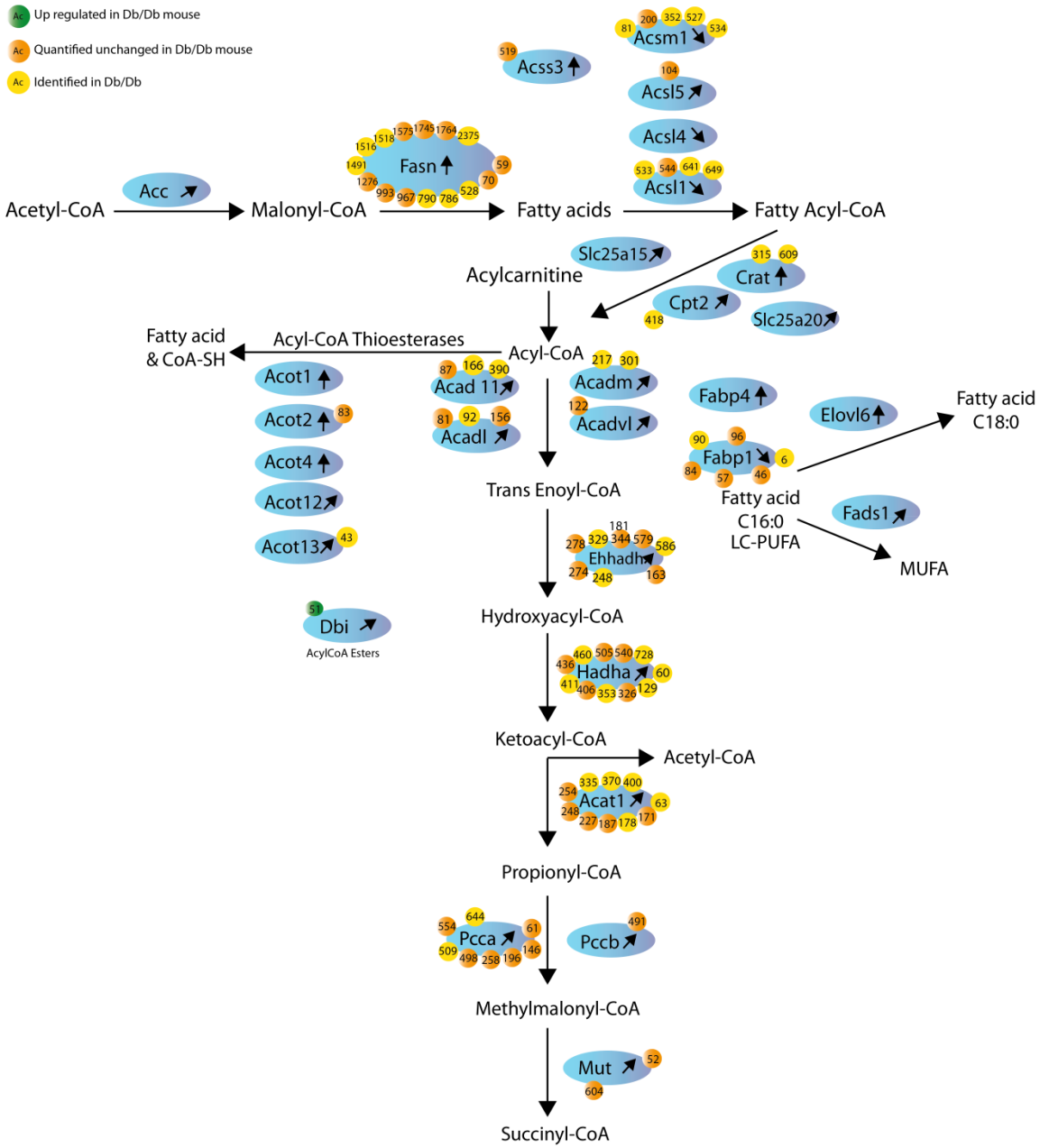

Figure 4: Modulation of the proteome and acetylome of the Fatty acid metabolism in the liver of Db/Db mice. Arrows indicate a significant up- or down-regulation of proteins in Db/Db mice. Acetylpeptides, which are significantly differently expressed, are colour coded: green indicates up-regulated, orange shows quantified unchanged sites and identified but not quantified sites are represented by yellow. Excess free fatty acids levels result in an elevated hepatic uptake and an up-regulation of several enzymes regulating the activation and the beta oxidation of fatty acids.

quantification. In total, we identified 1604 lysine acetylation sites (n=3) and the comparison of technical replicates showed an average Pearson correlation of 0.8 (**Suppl. Figure S2A**). Next, we performed a principle component analysis and detected a clear separation of component 1 (58%) and component 2 (20%) (**Suppl. Figure 2B**). When our acetylome data were compared to known acetylation sites from the phosphositeplus.org database 787 novel acetylation sites were identified. However, the statistical analysis and normalization to

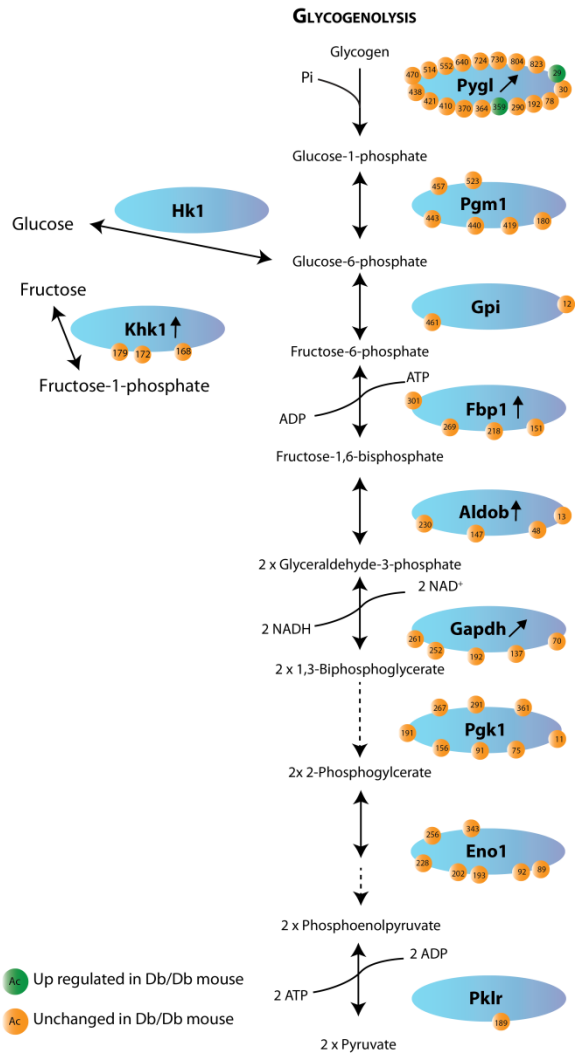

Figure 5: Diabetes-induced modulation of the proteome and acetylome of the carbohydrate metabolism in the liver of Db/Db animals. Arrows indicate a significant up or down regulation. Acetyl peptides which are significantly differently expressed are colour coded: green indicates upregulated acetyl sites (>1.5 fold change) and unchanged sites are represented by orange. When energy is required, glycogen is converted into glucose, via glycogenolysis, which is controlled by insulin. Type 2 diabetes is characterized by insulin resistance, resulting in elevated blood glucose levels.

protein ratios revealed a significant regulation for only 34 sites (fold change >1.5 and FDR < 0.05) (**Figure 6C, D, Table 1**). Eight of these acetylation sites present on seven proteins showed increased acetylation while 26 sites on 21 proteins were hypoacetylated in Db/Db animals. For example, we identified five acetylation sites on the cytosolic acyl-binding protein (Acbp, also known as Dbi, Diazepam binding protein), which has a high affinity for long chain acyl-CoA´s. Four of these acetylation sites (K8, K55, K61 and K77) were not regulated while K51 showed a two-fold increase in Db/Db animals. The crystal structure revealed that Acbp consists of a four-helix bundle fold and the residues Y29, K33, and K55 in the helix two and three are important binding sites for the 3´-phosphate AMP moiety of the CoA[40]. Thus, we assume that the K51 acetylation, which is in close proximity of these important residues for CoA binding, plays a role for the modulation of the CoA binding efficiency resulting from structural destabilization or charge neutralization.

We further found 19 acetylation sites on glycogen phosphorylase (Pygl) and three of them (K290, K370, K514) were not described previously. After normalization for the Pygl protein (~1.7 fold change up in Db/Db) we calculated a ~two-fold up-regulation for the K29 and K359 acetylation, indicating that these sites are potential targets for the enzymatic activity and/or stability of Pygl during chronic obesity and insulin resistance. Previous reports showed elevated protein levels together with increased Pygl activity in Db/Db mutants. Based on turnover data it was suggested that increased Pygl abundance in Db/Db animals can be explained by a decreased degradation rate[41]. Thus, the detection of two increased Pygl acetylation sites in Db/Db animals could reflect a potential protection against proteasomal degradation.

Another important metabolic enzyme is the mitochondrial Hydroxymethyl-glutaryl-CoA synthase (Hmgcs2), which was recently described as a potential target for Sirt3[19]. Since we found a ~two-fold increase of Hmgcs2 protein level in Db/Db animals, the protein normalization revealed a ~two-fold up-regulation only for the K310 in Db/Db animals whereas the other three detected acetylated lysines (K83, K243, K350) were not changed. Notably, it was shown that the K310 residue is responsible for the correct protein conformation and protein activity, supporting the conclusion that hyperacetylation of K310 is a specific response to altered metabolic conditions such as overnutrition and insulin resistance in Db/Db animals[19].

The highest change in acetylation were found for the K169 (a ~five-fold increased acetylation level) in the monooxygenase cytochrome P450 4A14, which was also increased at the protein level in Db/Db mice. Interestingly, a global ubiquitylation study of several mouse tissues showed that K169 was exclusively ubiquitylated in liver tissue[42]. We hypothesize that the dynamic acetylation of the P450 4A14 K169 is a liver specific response to increased metabolic and oxidative stress to hamper protein ubiquitylation.

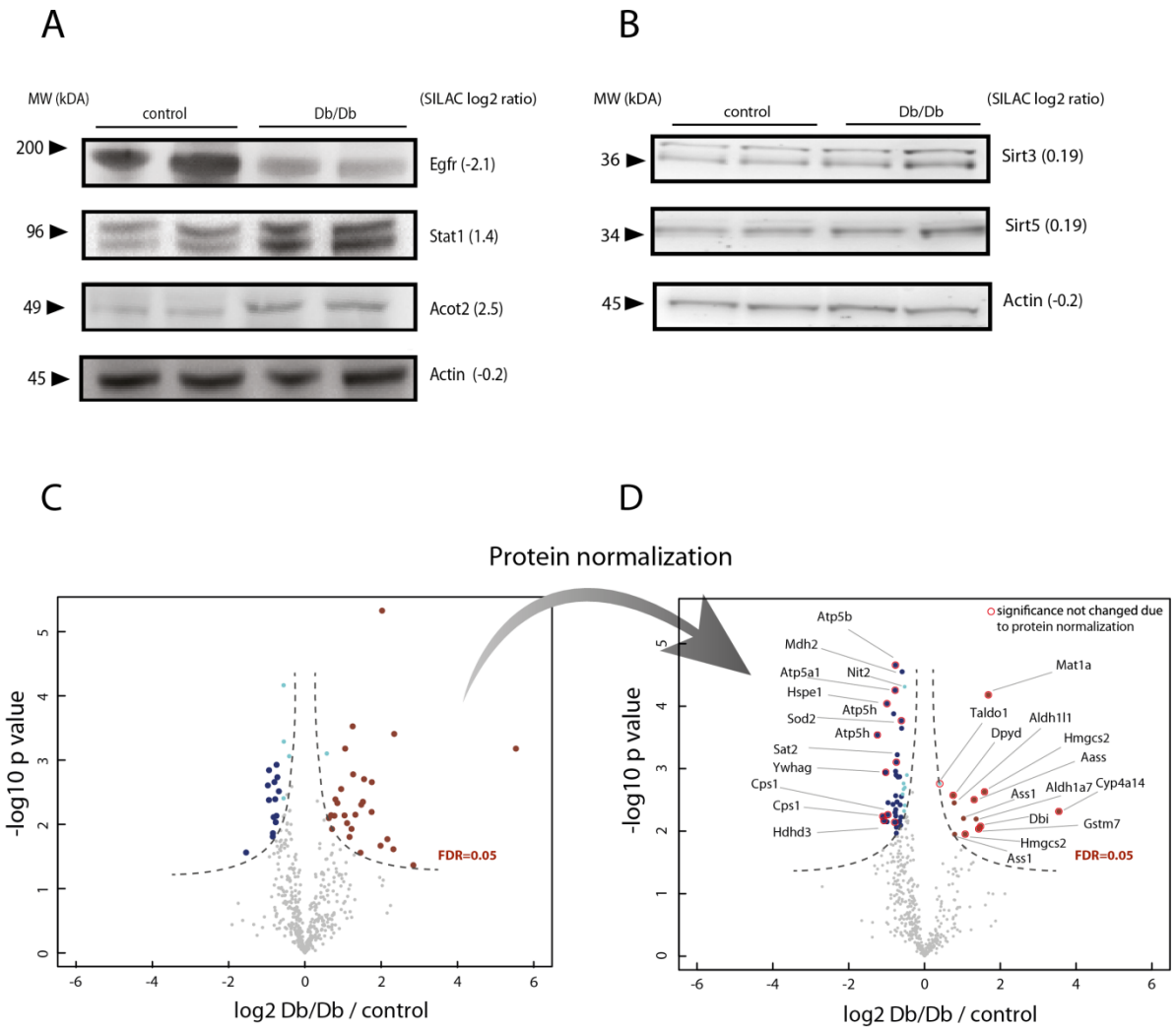

Figure 6: Alteration of the acetylation pattern by protein normalization and immunoblotting verification of selected candidates from control and Db/Db liver lysate. (A) Western blot conformation for down regulated epidermal growth factor receptor (Egfr), up regulated signal transducers and activators of transcription (Stat1) and acyl-CoA thioesterase (Acot2) including the log2 Ratio [DbDb/Ctrl] from the mass spectrometry proteome measurements. (B) Western blot analysis showed no changes for Sirt3 and Sirt5 between Db/Db and lean control animals including the log2 Ratio [DbDb/Ctrl] from the mass spectrometry proteome measurements. (C) Volcano plot of log2 ratios representing the log2 fold change of acetylation sites of Db/Db to control mice (FDR threshold 0.05, indicated by dashed line). Significant differently expressed acetylation sites are colour coded: red indicates up regulated proteins (>1.5 fold change), blue shows down regulated proteins (<0.75 fold change) and teal represents all proteins with lower absolute fold changes. (D) Effect of protein normalization on differentially acetylated peptides. Unaffected acetylated sites remaining significantly changed are indicated with a red border.

Energy is mainly produced within mitochondria and the activities of mitochondrial chain complexes are the building blocks to produce energy in form of ATP. An essential carrier to transport ATP from the mitochondrial matrix to the cytosol is the transmembrane protein ADP/ATP translocase 1 (Slc25a4, also known as Ant1). Slc25a4 deficient mice exhibit a severe mitochondrial myopathy and cardiomyopathy reflecting the importance of this ATP/ADP carrier system for the energy production [43]. Moreover, it was shown that increased levels of intracellular long chain fatty acids (LCFA-CoA) cause an inhibition of Scl25a4 carrier resulting in an elevated ADP level. The excess of ADP is levelled out by the activity of the adenylate kinase, which generates one molecule of ATP and AMP each from two ADP molecules. Subsequently, AMP is then converted by dephosphorylation into the purine nucleoside adenosine (ADO) and an increased level of intracellular ADO levels impairs the diffusion of extracellular ADO into the cell. A systematic increase in ADO results finally in pathophysiological insulin resistance effects, including increased extracellular urate concentration, increased ROS levels, and hypertension[44, 45]. Our study revealed a clear up-regulation of the acetylation of Scl25a4 at position K92 within the second transmembrane domain

in Db/Db animals. So far 15 acetylation sites in human and mouse Scl25a4 proteins were identified but our study showed for the first time the presence of a regulatory acetylation site on the Scl25a4 protein upon insulin resistance.

In addition to the hyperacetylated sites, we found 19 peptides originating from 15 mitochondrial proteins with a reduced acetylation level. We found a two-fold down-regulation for a single lysine residue each in the ATP synthase subunit alpha (Atp5a1-K539) and beta (Atp5b-K522) in Db/Db animals. Both sites were also detected in a recent study on Sirt3 deficient liver tissue but without any regulation, indicating that these sites are hypothetically the targets of other deacetylases such as Sirt5. Notably, the expression of the mitochondrial sirtuins Sirt3 and Sirt5 were not changed between Db/Db and lean controls (**Figure 6B**). Beside the two identified regulated lysines, no further acetylation changes were detected on additionally identified 65 acetylation sites on several ATP synthase subunits.

Among further identified hypoacetylated proteins we found two acetylation sites (K428 and K443) of the Aldehyde dehydrogenase (Aldh2) with a ~two-fold down-regulation in Db/Db animals. Similar to the cytochrome P450 family, Aldh2 acts mainly as a detoxification enzyme and is responsible for the conversion of biogenic and xenogenic aldehydes. Interestingly, Aldh2 has emerged as a protective enzyme against oxidative stress in the heart and studies on rats showed that Aldh2 activity may be responsible for the diabetes phenotype[46,47]. Whether the decreased acetylation has an impact on the Aldh2 activity or substrate affinity remains to be elucidated.

We further found two members of the TCA cycle, the malate dehydrogenase (Mdh2, K314) and fumarate hydratase (Fh, K63) with a reduced acetylation in Db/Db animals. In addition, the aspartate aminotransferase mAST (Got2), which (together with Mdh2) plays an important role for the regeneration of NADH inside the mitochondrial matrix, was also less acetylated. Previous studies showed Mdh2 activity concomitant with acetylation levels. The lysine sites K185, K301, K307 and K314, increase in response to food uptake[36]. In contrast, a Sirt3 dependent deacetylation of K239 of the Mdh2 enzyme was shown upon feeding[48]. Here, we found a slight down-regulation of K314 on Mdh2 in Db/Db animals, whereas the acetylation K301 was not changed. Thus, our data showed a potential role for Mdh2 K314 acetylation site to modulate the metabolic activity of the TCA cycle upon chronic obesity. The remaining hypoacetylated lysine residues identified in this study were found on a few key enzymes involved in the metabolic pathways located in mitochondria. The carbamoyl-phosphate synthase Cps1 is one of the most abundant liver enzymes. It catalyses the fusion of ammonia and bicarbonate ion to carbamoyl-phosphate and plays therefore a crucial role in nitrogen detoxification. Here, we observed 36 known acetylation sites on Cps1 and additionally 4 sites (K176, K399, K906, K934), which were not previously described. Moreover, we found two sites on Cps1 (K55 and K915) with a decreased acetylation level in Db/Db animals.

Another acetylation changes were found in the liver-type glutaminase (Gls2), an important transamination enzyme, which converts glutamine to glutamate providing then alpha Ketoglutarat for further metabolic steps. Glutaminases play also a role in regulating the sensitivity to reactive oxygen species (ROS) and cell apoptosis[49]. The Gls2 enzyme was detected with two acetylation sites (K91 and K240) with a reduced acetylation level in Db/Db animals for K91 only. Further, the highly acetylated glutamate dehydrogenase Glud1 was detected with 15 acetylation sites and showed decreased acetylation levels in Db/Db animals only for K162 and K415. In contrast, we have not observed any changes in the acetylation of the five lysine residues detected in the ornithine carbaxoyltransferase (Oct1).

Summing up, we identified down regulation of specific acetylation sites on several enzymes involved in nitrogen metabolism most likely reflecting the adaption of Db/Db animals to increased protein breakdown and amino acid catabolism.

Conclusions

Large-scale proteomic analysis of animal models has shown that development of the metabolic syndrome under pathological conditions is tightly correlated with alterations of signaling pathways, mitochondrial activity, and oxidative stress. Moreover, functional studies have also pointed out that enzymes, which are involved in carbohydrate and lipid metabolism are acetylated on lysine residues and the site occupancy has a pronounced effect on the activity of those enzymes.

Swiss-Prot.	Gene	Protein	Site [K]	ratio Protein	ratio Peptide	Function
Mitochondrial upregulated				log2	log2	
D3Z563	Dbi	Acyl-CoA-binding protein	51	0.43	1.32	Fatty-acyl CoA binding
P54869	Hmgcs2	Hydroxymethylglutaryl-CoA synth.	310	1.19	1.15	Lipid metabolism
Q9ET01	Pygl	Glycogen phosphorylase	29	0.73	1.02	Carbohydrate metabolism
			359		0.82	
P48962	Slc25a4	ADP/ATP translocase 1	92	-0.81	0.92	Transport
Q80W21	Gstm7	Glutathione S-transferase Mu 7	272	-0.05	0.81	Detoxyfication
Mitochondrial downregulated						
G5E8N5	Ldha	L-lactate dehydrogenase	86	0.49	-0.83	Glycolysis
Q571F8	Gls2	Glutaminase 2	91	-0.33	-0.74	Glutamine catabolism
Q8QZV3	Eci1	Enoyl-CoA delta isomerase 1	76	0.26	-0.65	Lipid metabolism
Q8C196	Cps1	Carbamoyl-phosphate synthase	55	-0.33	-0.64	Urea cycle
			915		-0.61	
Q99K67	Aass	α-aminoadipic semialdehyde synth.	286	1.18	-0.56	Lysine degradation
Q9DBT9	Dmgdh	Dimethylglycine dehydrogenase	107	0.45	-0.51	Aminomethyltransferase
			427		-0.45	
P26443	Glud1	Glutamate dehydrogenase 1	162	0.26	-0.51	Transamination
			415		-0.44	
Q03265	Atp5a1	ATP synthase a	539	-0.04	-0.51	ATP Synthesis
P56480	Atp5b	ATP synthase subunit b	522	-0.06	-0.50	ATP Synthesis
P47738	Aldh2	Aldehyde dehydrogenase 2	428	0.23	-0.39	Aldehyde dehydrogenase
			443		-0.56	
P08249	Mdh2	Malate dehydrogenase	314	0.15	-0.49	TCA cycle
P97807	Fh	Fumarate hydratase	63	0.24	-0.48	TCA cycle
E9QNP7	Gm4952	Glycine N-acyltransferase-like prot.	183	-0.02	-0.46	Acyltransferase
P09671	Sod2	Superoxide dismutase	68	0.01	-0.42	Oxidoreductase
P05202	Got2	Aspartate aminotransferase	296	0.25	-0.39	Aminotransferase
Cytoplasm downregulated						
P61982	Ywhag	14-3-3 protein gamma	162	0.16	-0.96	Insulin signaling
Q6P8J2	Sat2	Diamine acetyltransferase 2	29	0.00	-0.56	Diamine N-acetyltransferase
Q3U367	Aldh9a1	Aldehyde dehydrogenase 9A1	54	0.21	-0.48	Carnitine metabolic process
Q9JHW2	Nit2	Omega-amidase NIT2	68	0.17	-0.41	Nitrogen & sulfur metabolism
Nuclear & ER upregulated						
P42669	Pura	Transcriptional activator protein Pur-α	272	-0.05	0.81	Transcription activator
O35728	Cyp4a14	Cytochrome P450 4A14	169	3.14	2.40	Detoxyfication
downregulated Nuclear						
P62806	Hist1h4a	Histone H4	13	0.00	-0.63	Nucleosome asembly
			17		-0.78	
Q9D0J8	Ptms	Parathymosin	15	0.32	-0.48	Immune systeme

Table 1: Significantly regulated acetylation sites after normalization to protein ratio in Db/Db mice.

Here we applied an in-vivo SILAC approach and quantified more than 5000 proteins in liver tissue of insulin resistance Db/Db animals. We found significant changes of more than 1.5 fold in 237 proteins, which reflected the metabolic adaption to increased carbohydrate and lipid metabolism and changes of several receptors and signaling molecules. In addition, the immunopurification of acetyl-lysine residues allowed us to quantify more than 1600 acetylated peptides with a fraction of 34 regulated sites in Db/Db animals. Importantly, the combination of accurate protein and acetyl-lysine peptide SILAC ratios allowed

us to normalize modified peptides and to monitor acetylation changes with high assurance. For example, we found initially a four-fold enrichment of K235 of the methionine adenosyltransferase Mat1a, which is a central enzyme for the synthesis of S-adenosylmethionine (SAM). The normalization to the Mat1a protein level, which was also three-fold up-regulated in Db/Db animals, resulted finally in an equal ratio between Db/Db and lean controls. Similarly, we corrected six acetyl lysine sites on Cps1, which initially appeared to be up-regulated but the protein normalization led to an equal distribution of those sites. Thus, the simultaneous quantification of protein and modified peptide ratios is crucial for the correct assessment of peptides with a posttranslational modification regulated under pathological conditions.

Our report presents the first quantified, comprehensive proteomic analysis combining proteome and acetylome of the liver of Db/Db mice. Two recent reports used fractions from the membrane and endoplasmatic reticulum to analyse the proteome changes in Db/Db animals[50] [51]. Although they found similar pathways to be regulated, the overall overlap to our data set was rather low. Kim et al. found 33 proteins, which were increased in Db/Db animals. Although we achieved a considerably higher coverage of quantified proteins, we found only eight overlapping candidates with the Kim et al. dataset in Db/Db animals. The reason for this discrepancy is most likely due to the isolation of a specific cellular compartment by Kim et al. compared to our global approach.

The comparison to a recent deep sequencing dataset revealed a reasonable Pearson correlation of 0.6 for the class of regulated candidates. Considering the overlapping proteins from the deep sequencing analysis and our proteome study we found 178 down regulated proteins in Db/Db animals. On mRNA level 57 genes are equally down regulated and for 83 genes we did not find any changes on mRNA levels in Db/Db animals. For example, we detected four signal recognition particles (Srp) Srp9, Srp19, Srp68, and Srp72 to be down regulated on protein level with no corresponding changes on the mRNA level. Those ribonucleoprotein complexes play an essential role to mediate co-translational transport of proteins to the endoplasmatic reticulum or plasma membrane. Our data present further evidence that this secretory complex is dysregulated in Db/Db animals by a significant down regulation of four further members, including the 60S ribosomal L3 (Rpl3), the signal peptidase complex 2 (Spc2), the translocon-associated protein (Ssr1), and the protein transport Sec61 (Sec61a1). The notion that serum proteins such as albumin, coagulation factors, major urinary proteins (Mup) and complement factors were also reduced on protein level in Db/Db animals favours a dysregulation on protein secretion from hepatocytes in Db/Db animals.

In the class of up regulated proteins we observed 280 candidates and the overlap to the mRNA data set revealed a congruent regulation for 159 mRNAs, whereas 103 candidates were not changed on mRNA level. Notably, several key enzymes of the lipid metabolism such as the fatty acid synthase (Fasn) and the Fatty acid-binding protein (Fabp4) were only up-regulated on protein level and with no changes on the transcript level for these genes. Similarly, the Glucose-6-phosphatase (G6pc2) and the Fructose-bisphosphate aldolase B (Aldob), two important enzymes of the gluconeogenesis, were only up-regulated on protein level but their corresponding mRNA was not changed. Thus, the combination of deep sequencing data and protein levels will assist to integrate post-transcriptional regulations with protein stabilities under pathological conditions.

Our acetyl-peptide screen in Db/Db and lean control animals emphasizes abundant acetylation in the fraction of mitochondrial proteins and not surprisingly we found acetyl-lysine residues in a large quantity on mitochondrial proteins, which are involved in energy metabolism, amino acid conversion and urea cycle. For example, the activity of the urea cycle protein Cps1, the key enzyme for the initial step of ammonia detoxification is regulated by the sirtuin family member Sirt5[52]. During fasting Sirt5 is activated by increased levels of NAD and leads to deacetylation of Cps1, which up-regulates its activity. Similar results were observed by the administration of a high protein diet where the urea cycle becomes also very important. Moreover, a study from Ogura et al. showed that the transgenic overexpression of Sirt5 in mice leads to decreased acetylation and increased Cps1 activity[53]. Here, we observed 36 acetylation sites on Cps1 but we found significantly decreased levels only for the sites K55 and K915 in Db/Db animals. Thus, the N-terminal (K55) site within the small subunit of carbamoyl phosphate synthase and/ or the (K915) site within the oligomerisation domain in the large subunit could play a pivotal role for the Cps1 activity. However, other reports found that Sirt5 activity was more related to succinylation compared to a relative poor activity as a deacetylase[54]. Alternatively, the mitochondrial Sirt3 could also be responsible for the deacetylation of Cps1. Western blot analysis showed no changes for Sirt3 and Sirt5 between Db/Db and lean control animals, suggesting most likely altered protein activities for these sirtuins (**Figure 6B**). It will be important to generate point mutations on K55 and K915 of Cps1 to gain more

insights into the functional relevance of these regulatory sites during obesity and insulin resistance.

Taken together, accurate SILAC quantification enabled us to monitor dynamic acetylation sites on mitochondrial, cytoplasmatic and nuclear proteins. Moreover, we observed acetylated peptides in several other pathways, including inflammatory processes, cell cycle regulation, and secretory pathways, suggesting that the extent of lysine acetylations is comparable to serine and threonine phosphorylations[55]. However, so far the function for most of those acetyl-lysine sites is completely unknown and our data set provide a recourse to study how protein acetylation regulate the activity of enzymes under insulin resistance conditions in living animals.

Experimental Procedure

Antibodies

Antibodies used for immunopurification were specific for polyclonal acetyl-lysine K(ac) (Immunechem Pharmaceuticals Inc., ICP0388). Antibodies for Western Blotting were purchased from Cell Signaling (pan actin #4968, Stat1 #9172, Egfr #2232, Sirt3 #D22A3, Sirt5 #D8C3) and Sigma Aldrich (Acot2 SAB2100030).

Animals

All procedures involving animals were performed in accordance with the guidelines for animal experimentation of the local authorities. All animals were kept on the identical C57BL/6J background. For this study only male mice were used from the Jackson laboratory.

Dissection of liver and lysis

After four hours fasting, mice were anesthetized via intraperitoneal injection of ketamine-xylazine solution (0.1 ml/10 g body weight). After perfusion with cold PBS, animals were euthanized by cervical dislocation. Liver tissue was harvested and snap frozen in liquid nitrogen.

Frozen liver tissue was cryogenically grinded with mortar and pestle and then suspended in lysis buffer (4% SDS in 0.1 M Tris/HCl pH 7.6) completed with protease inhibitor cocktail (Roche cOmplete tablets 1 tablet per 100 mL buffer). For complete cell lysis samples were heated for 10 minutes at 95°C. The homogenate was centrifuged at 16.000 g for ten minutes. Any lipids were removed from the top of the supernatant by aspiration.

In-gel digestion

For global proteome experiments the protein concentration of the liver lysates were measured by DC Protein assay (BioRad). Db/Db and control liver proteins were equally mixed with the liver lysate of the Lys6-labeled SILAC spike-in standard, respectively. Protein mixtures were separated according their molecular weight by subjecting them to SDS-PAGE (4-12% NuPage BisTris Gel, Invitrogen) followed by Colloidal Blue staining (Invitrogen). Gel lanes were cut into equal pieces and digested in gel as described by Shevchenko et al[56]. In brief, gel pieces were washed, de-stained and dehydrated. Proteins were reduced with 10 mM dithiothreitol (DTT), alkylated with 55 mM iodoacetamide (IAA) and digested with the endopeptidase LysC (Wako) overnight. Generated peptides were extracted using an increasing acetonitrile concentration. Collected peptide mixtures were concentrated and desalted using the Stop and Go Extraction (STAGE) technique[57].

Strong cation exchange chromatography

Protein mixtures were digested following the Filter Aided Sample Preparation (FASP)[58], generated peptides were acidified to pH 2.62 and the solution was adjusted to 30% acetonitrile. A Resource S (GE Healthcare) strong cation exchange column was used for charge based separation. Peptide mixture was loaded onto the column with running phase A (7 mM KH_2PO_4 in 30 % ACN pH=2.65). Eluting peptides along an increasing content of buffer B (7 mM KH_2PO_4, 350 mM KCL in 30 % ACN pH=2.65) were collected into ten fractions. Solutions were concentrated and desalted using STAGE technique prior mass spectrometric analysis.

Enrichment of acetylated peptides

For enrichment of acetylated peptides the Db/Db or control liver proteins were mixed with SILAC liver in a one to one ratio. Combined proteins mixtures were precipitated overnight using 4 volumes of ice-cold acetone. The protein pellet was dissolved in 6 M urea, 2 M thiourea, 10 mM HEPES, pH 8 and subjected to digestion in solution. Next, protein disulfide bonds were reduced with 10 mM dithiothreitol (DTT) and alkylated with 5.5 mM iodoacetamide. For the first digestion step LysC (Wako) (protein to LysC ratio = 100:1) was added for 3 hours. Then, the samples were diluted to 2 M urea with 50 mM ammonium bicarbonate, and sequencing-grade trypsin (Promega, Madison, WI) was added to the samples (protein to trypsin ratio = 100:1) overnight at room temperature. Digestions were quenched by TFA acidification, and desalted with a tC18 sep-Pak (Waters, 500 mg WAT036790). Peptides were eluted from the

column with 2 × 2 ml 50% acetonitrile/ 0.1% formic acid. Eluted peptide samples were placed in a vacuum concentrator to evaporate the elution solvent. K(ac) antibody beads were washed four times with immunoprecipitation buffer (50 mM MOPS pH 7.2, 10 mM Sodium Phosphate (Na_3PO_4) and 50 mM NaCl) on ice. 20 mg of peptide sample was incubated with 50 µL K(ac) antibody overnight by end-over-end rotation at 4°C. Finally, K(ac) enriched peptides were washed, eluted with 0.1% TFA and desalted with the STAGE technique.

Western Blotting

For Western blot analyiss 20 µg of lysed liver tissue were separated according to their molecular weight using 4-12% NuPage BisTris Gel (Invitrogen) and blotted on nitrocellulose membranes. Selected antibodies were incubated following manufacturer's recommendations. Development was done using Western Lightening Ultra (Perkin Elmer, Inc.) and recording in a VersaDoc MP (BioRad) using default settings.

Liquid Chromatography and Mass Spectrometry

A binary buffer system consisting of buffer A (0.1% formic acid or 0.5% acetic acid) and buffer B (80% Acetonitrile, 0.1% formic acid or 0.5% acetic acid) was used for peptide separation on an Easy nano-flow HPLC system (Thermo Fisher Scientific). This system was coupled via a nano electrospray ionization source to the QExactive or LTQ Orbitrap Velos mass spectrometer. Peptide elution from the in-house packed 20 cm (3 µm Beads, 75 µm ID, Dr. Maisch Germany) or 50 cm (1.8 µm Beads, 75 µm ID, Dr. Maisch Germany) column was achieved by increasing the relative amount of B from 7% to 38% in a linear gradient within 150 min or 240 min at a column temperature of 40°C. Followed by 5 min at 95% B and gradients were completed by re-equilibration time of 5 min to 5% B.

QExactive

MS Spectra were recorded at 70,000 resolution (200 m/z, 3E6 ions as AGC target) within a maximum injection time of 20 ms. Acquisition of MS/MS spectra in a data-dependent mode after HCD fragmentation (Top10) was carried out at 17,500 (200 m/z) in the highly accurate Orbitrap mass analyzer using 1E6 as the AGC target and 60 ms for maximal injection time. Separation width was set to 1.7 m/z.

LTQ Orbitrap Velos

For the analysis we used a combination of 1D-Gel and mass spectrometry. For the experiments we used a LTQ Orbitrap Velos with a Top15 (CID) method. Collision energy for collision induced dissociation was set to 35. AGC target for acquiring MS spectra and MS^2 spectra was set to 1E6 and 3E4, respectively.

Data Processing and Analysis

All acquired raw file were processed using MaxQuant 1.3.7.4 as well as the implemented Andromeda search engine. For protein identification HCD MS/MS Spectra were correlated and compared to the latest Uniprot mouse (Mus musculus) data set involving 74,265 protein sequence entries. An additional list of common contaminants was used, addressing the filtering of those proteins. Searches were performed with tryptic or LysC specificity allowing two miss cleavages and a mass range window of 4.5 ppm for MS spectra. For first MS/MS searches we allowed a mass range of 7 ppm and for main searches 4 ppm. Carbamidomethyl at cysteine residues was set as a fixed modification. Oxidation at methionine, acetylation at the N- terminus and lysine acetylation were considered as variable modifications. PSM (peptide spectrum match) and protein FDR were set to 0.01 and the minimal peptide length to 7 amino acids. For SILAC quantification the minimal ratio count was set to 2.

Perseus was used for following data analysis and visualization as well as the statistical environment R. Distance matrix for hierarchical clustering was computed by pearson correlation and for clustering the average linkage method was used. Heatmap was generated using gplots Package [59].

Addressing the multiple testing problem, FDR was controlled using a smiliar approach as SAM (statistical analysis of microarray) described by Tusher et al. [60]. This technique was originally developed for microarray but was shown to lead to sufficient results for proteomic datasets. R package *siggenes* [61] [62] from bioconductor was used and p0 (priori probability) was calculated by default settings. The fudge value s0 was set to 0.1 and equal variance was assumed. Significance change was considered for FDR threshold of 0.05 (number of permutations: 1000) by applying an appropriate value for delta.

To determine the distribution of experimental groups, a principal component analysis (PCA) was performed using Perseus.

Acknowledgements

The authors would like to thank Sylvia Jeratsch, Tanja Piller for excellent technical assistants and Alejandro Carpy for discussions.

Notes and references

† Equal contributions to this paper

[a] Max Planck Institute for Heart and Lung Research, Parkstr. 1, 61231 Bad Nauheim, Germany

[b] Correspondence should be addressed to Marcus Krüger, E-mail: marcus.krueger@mpi-bn.mpg.de. Fax: +49(0)6032705419. Tel: +49(0)60327051760.

[#] present address: Excellence Cluster, Cellular Stress Responses in Aging –Associated Diseases, CECAD, Institute for Genetics, University of Cologne, Joseph-Stelzmann-Straße 26, 50931 Köln

† Electronic Supplementary Information (ESI) available: Figure S1-S2, Table 1-4.

References

1. B. Cheatham and C. R. Kahn, *Endocr Rev*, 1995, **16**, 117-142.
2. C. M. Taniguchi, B. Emanuelli and C. R. Kahn, *Nat Rev Mol Cell Biol*, 2006, **7**, 85-96.
3. A. R. Vaquero, N. E. Ferreira, S. V. Omae, M. V. Rodrigues, S. K. Teixeira, J. E. Krieger and A. C. Pereira, *Physiol Genomics*, 2012, **44**, 903-914.
4. F. Zhang, X. Xu, Y. Zhang, B. Zhou, Z. He and Q. Zhai, *PLoS One*, 2013, **8**, e57766.
5. P. Zimmet and C. R. Thomas, *J Intern Med*, 2003, **254**, 114-125.
6. M. A. Lazar, *Science*, 2005, **307**, 373-375.
7. C. Postic and J. Girard, *J Clin Invest*, 2008, **118**, 829-838.
8. M. Lu, M. Wan, K. F. Leavens, Q. Chu, B. R. Monks, S. Fernandez, R. S. Ahima, K. Ueki, C. R. Kahn and M. J. Birnbaum, *Nat Med*, 2012, **18**, 388-395.
9. C. M. Taniguchi, K. Ueki and R. Kahn, *J Clin Invest*, 2005, **115**, 718-727.
10. B. B. Lowell and G. I. Shulman, *Science*, 2005, **307**, 384-387.
11. R. N. Bergman and M. Ader, *Trends Endocrinol Metab*, 2000, **11**, 351-356.
12. J. R. Peinado, A. Diaz-Ruiz, G. Fruhbeck and M. M. Malagon, *Proteomics*, 2014, **14**, 452-466.
13. H. Chen, O. Charlat, L. A. Tartaglia, E. A. Woolf, X. Weng, S. J. Ellis, N. D. Lakey, J. Culpepper, K. J. Moore, R. E. Breitbart, G. M. Duyk, R. I. Tepper and J. P. Morgenstern, *Cell*, 1996, **84**, 491-495.
14. W. J. Roesler, S. Pugazhenthi and R. L. Khandelwal, *Mol Cell Biochem*, 1990, **92**, 99-106.
15. P. Nagarajan, M. J. Mahesh Kumar, R. Venkatesan, S. S. Majundar and R. C. Juyal, *World J Gastroenterol*, 2012, **18**, 1141-1153.
16. Q. M. Anstee and R. D. Goldin, *Int J Exp Pathol*, 2006, **87**, 1-16.
17. S. Kim, I. Sohn, J. I. Ahn, K. H. Lee and Y. S. Lee, *Gene*, 2004, **340**, 99-109.
18. H. Lan, M. E. Rabaglia, J. P. Stoehr, S. T. Nadler, K. L. Schueler, F. Zou, B. S. Yandell and A. D. Attie, *Diabetes*, 2003, **52**, 688-700.
19. T. Shimazu, M. D. Hirschey, L. Hua, K. E. Dittenhafer-Reed, B. Schwer, D. B. Lombard, Y. Li, J. Bunkenborg, F. W. Alt, J. M. Denu, M. P. Jacobson and E. Verdin, *Cell Metab*, 2010, **12**, 654-661.
20. M. Kruger, M. Moser, S. Ussar, I. Thievessen, C. A. Luber, F. Forner, S. Schmidt, S. Zanivan, R. Fassler and M. Mann, *Cell*, 2008, **134**, 353-364.
21. C. M. Kusminski, S. Shetty, L. Orci, R. H. Unger and P. E. Scherer, *Apoptosis*, 2009, **14**, 1484-1495.
22. M. Febbraio, N. A. Abumrad, D. P. Hajjar, K. Sharma, W. Cheng, S. F. Pearce and R. L. Silverstein, *J Biol Chem*, 1999, **274**, 19055-19062.
23. A. Ibrahimi, A. Bonen, W. D. Blinn, T. Hajri, X. Li, K. Zhong, R. Cameron and N. A. Abumrad, *J Biol Chem*, 1999, **274**, 26761-26766.
24. J. L. Lam, Y. Jiang, T. Zhang, E. Y. Zhang and B. J. Smith, *Drug Metab Dispos*, 2010, **38**, 2252-2258.
25. C. Wiesinger, M. Kunze, G. Regelsberger, S. Forss-Petter and J. Berger, *J Biol Chem*, 2013, **288**, 19269-19279.
26. I. Shimomura, K. Tokunaga, S. Jiao, T. Funahashi, Y. Keno, T. Kobatake, K. Kotani, H. Suzuki, T. Yamamoto, S. Tarui and et al., *Biochim Biophys Acta*, 1992, **1124**, 112-118.
27. D. G. Mashek, L. O. Li and R. A. Coleman, *J Lipid Res*, 2006, **47**, 2004-2010.
28. J. D. Hayes and D. J. Pulford, *Crit Rev Biochem Mol Biol*, 1995, **30**, 445-600.
29. S. S. Mastana, A. Kaur, R. Hale and M. R. Lindley, *Mol Biol Rep*, 2013.
30. S. B. Jadhao, R. Z. Yang, Q. Lin, H. Hu, F. A. Anania, A. R. Shuldiner and D. W. Gong, *Hepatology*, 2004, **39**, 1297-1302.
31. G. S. Hotamisligil and E. Erbay, *Nat Rev Immunol*, 2008, **8**, 923-934.
32. P. J. Miettinen, J. Ustinov, P. Ormio, R. Gao, J. Palgi, E. Hakonen, L. Juntti-Berggren, P. O. Berggren and T. Otonkoski, *Diabetes*, 2006, **55**, 3299-3308.
33. W. Cai, J. C. He, Z. Zhu, C. Lu and H. Vlassara, *PNAS*, 2006, **103**, 13801-13806.
34. P. A. Grimsrud, J. J. Carson, A. S. Hebert, S. L. Hubler, N. M. Niemi, D. J. Bailey, A. Jochem, D. S. Stapleton, M. P. Keller, M. S. Westphall, B. S. Yandell, A. D. Attie, J. J. Coon and D. J. Pagliarini, *Cell Metab*, 2012, **16**, 672-683.
35. A. S. Hebert, K. E. Dittenhafer-Reed, W. Yu, D. J. Bailey, E. S. Selen, M. D. Boersma, J. J. Carson, M. Tonelli, A. J. Balloon, A. J. Higbee, M. S. Westphall, D. J. Pagliarini, T. A. Prolla, F. Assadi-Porter, S. Roy, J. M. Denu and J. J. Coon, *Mol Cell*, 2013, **49**, 186-199.
36. S. Zhao, W. Xu, W. Jiang, W. Yu, Y. Lin, T. Zhang, J. Yao, L. Zhou, Y. Zeng, H. Li, Y. Li, J. Shi, W. An, S. M.

Hancock, F. He, L. Qin, J. Chin, P. Yang, X. Chen, Q. Lei, Y. Xiong and K. L. Guan, *Science*, 2010, **327**, 1000-1004.

37. M. D. Hirschey, T. Shimazu, J. Y. Huang and E. Verdin, *Methods Enzymol*, 2009, **457**, 137-147.
38. A. A. Kendrick, M. Choudhury, S. M. Rahman, C. E. McCurdy, M. Friederich, V. H. J.L., W. P.A., B. N., B. J., G. D., S. M.N., J. E., K. C.R., F. J.E. and J. K.R., *Biochem J*, 2011, **433(3):505-14**, 505-514.
39. M. J. Rardin, J. C. Newman, J. M. Held, M. P. Cusack, D. J. Sorensen, B. Li, B. Schilling, S. D. Mooney, C. R. Kahn, E. Verdin and B. W. Gibson, *Proc Natl Acad Sci U S A*, 2013, **110**, 6601-6606.
40. J. P. Taskinen, D. M. Aalten, J. Knudsen and R. K. Wierenga, *Proteins: Structure, Function, and Bioinformatics*, 2007, **66**, 229-238.
41. W. J. Roesler, M. S. Nijjar and R. L. Khandelwal, *Mol Cell Biochem*, 1989, **87**, 147-152.
42. S. A. Wagner, P. Beli, B. T. Weinert, C. Scholz, C. D. Kelstrup, C. Young, M. L. Nielsen, J. V. Olsen, C. Brakebusch and C. Choudhary, *Mol Cell Proteomics*, 2012, **11**, 1578-1585.
43. B. H. Graham, K. G. Waymire, C. B., T. I.A., M. G.R. and W. D.C., *Nature Genetics*, 1997, **16**, 226–234.
44. S. J. Bakker, J. C. ter Maaten, C. Popp-Snijders, J. P. Slaets, R. J. Heine and R. O. Gans, *J Clin Endocrinol Metab*, 2001, **86**, 1206-1211.
45. J. Ciapaite, S. J. Bakker, V. E. G., W. M.J., T. T., S. C.G., F. M., O. D.M., D. M., H. R.J., W. H.V. and K. K., *Biochim Biophys Acta*, 2007, **1772**, 307-316.
46. C. H. Chen, G. R. Budas, E. N. Churchill, D. M.H., H. T.D. and M.-R. D., *Science*, 2008, **321**, 1493-1495.
47. Q. Zhang, Y. Lu, Y. Ding, J. Zhai, Q. Ji, W. Ma, M. Yang, H. Fan, J. Long, Z. Tong, Y. Shi, Y. Jia, B. Han, W. Zhang, C. Qiu, X. Ma, Q. Li, Q. Shi, H. Zhang, D. Li, J. Zhang, J. Lin, L. Y. Li, Y. Gao and Y. Chen, *J Med Chem*, 2012, **55**, 8757-8769.
48. A. J. Still, B. J. Floyd, A. S. Hebert, C. A. Bingman, J. J. Carson, D. R. Gunderson, B. K. Dolan, P. A. Grimsrud, K. E. Dittenhafer-Reed, D. S. Stapleton, M. P. Keller, M. S. Westphall, J. M. Denu, A. D. Attie, J. J. Coon and D. J. Pagliarini, *J Biol Chem*, 2013, **288**, 26209-26219.
49. J. M. Mates, J. A. Segura, M. Martin-Rufian, J. A. Campos-Sandoval, F. J. Alonso and J. Marquez, *Curr Mol Med*, 2013, **13**, 514-534.
50. G. H. Kim, E. C. Park, S. H. Yun, Y. Hong, D. G. Lee, E. Y. Shin, J. Jung, Y. H. Kim, K. B. Lee, I. S. Jang, Z. W. Lee, Y. H. Chung, J. S. Choi, C. Cheong, S. Kim and S. I. Kim, *Proteomics*, 2013, **13**, 1164-1179.
51. E. C. Park, G. H. Kim, S. H. Yun, H. L. Lim, Y. Hong, S. O. Kwon, J. Kwon, Y. H. Chung and S. I. Kim, *Int J Mol Sci*, 2012, **13**, 17230-17243.
52. T. Nakagawa, D. J. Lomb, M. C. Haigis and L. Guarente, *Cell*, 2009, **137**, 560-570.
53. M. Ogura, Y. Nakamura, D. Tanaka, X. Zhuang, Y. Fujita, A. Obara, A. Hamasaki, M. Hosokawa and N. Inagaki, *Biochem Biophys Res Commun*, 2010, **393**, 73-78.
54. M. J. Rardin, W. He, Y. Nishida, J. C. Newman, C. Carrico, S. R. Danielson, A. Guo, P. Gut, A. K. Sahu, B. Li, R. Uppala, M. Fitch, T. Riiff, L. Zhu, J. Zhou, D. Mulhern, R. D. Stevens, O. R. Ilkayeva, C. B. Newgard, M. P. Jacobson, M. Hellerstein, E. S. Goetzman, B. W. Gibson and E. Verdin, *Cell Metab*, 2013, **18**, 920-933.
55. A. Lundby, K. Lage, B. T. Weinert, D. B. Bekker-Jensen, A. Secher, T. Skovgaard, C. D. Kelstrup, A. Dmytriyev, C. Choudhary, C. Lundby and J. V. Olsen, *Cell Rep*, 2012, **2**, 419-431.
56. A. Shevchenko, H. Tomas, J. Havlis, J. V. Olsen and M. Mann, *Nat Protoc*, 2006, **1**, 2856–2860
57. J. Rappsilber, Y. Ishihama and M. Mann, *Anal. Chem.* , 2003, **75**, 663–670.
58. J. R. Wiśniewski, A. Zougman and M. Mann, *J Proteome Res*, 2009, **8**, 5674-5678.
59. G. R. Warnes, B. Bolker, L. Bonebakker, R. Gentleman, W. H. A. Liaw, T. Lumley, M. Maechler, A. Magnusson, S. Moeller, M. Schwartz and B. Venables, 2013.
60. V. G. Tusher, R. Tibshirani and G. Chu, *Proc Acad Nat Sci*, 2001, **98**, 5116-5121.
61. H. Schwender, 2012.
62. H. Schwender, A. Krause and K. Ickstadt, *RNews*, 2006, **6**, 45-50.